EOS *Terra* Aerosol and Radiative Flux Validation: An Overview of the Chesapeake Lighthouse and Aircraft Measurements for Satellites (CLAMS) Experiment

W. L. SMITH JR.,* T. P. CHARLOCK,* R. KAHN,+ J. V. MARTINS,#,++ L. A. REMER,# P. V. HOBBS,@ J. REDEMANN,& AND C. K. RUTLEDGE**

*Atmospheric Sciences Competency, NASA Langley Research Center, Hampton, Virginia
+Jet Propulsion Laboratory, California Institute of Technology, Pasadena, California
#Laboratory for Atmospheres, NASA Goddard Space Flight Center, Greenbelt, Maryland
@Department of Atmospheric Sciences, University of Washington, Seattle, Washington
&Bay Area Environmental Research Institute, Sonoma, California
**Analytical Services and Materials, Inc., Hampton, Virginia

(Manuscript received 26 May 2004, in final form 25 August 2004)

ABSTRACT

NASA developed an Earth Observing System (EOS) to study global change and reduce uncertainties associated with aerosols and other key parameters controlling climate. The first EOS satellite, *Terra*, was launched in December 1999. The Chesapeake Lighthouse and Aircraft Measurements for Satellites (CLAMS) field campaign was conducted from 10 July to 2 August 2001 to validate several *Terra* data products, including aerosol properties and radiative flux profiles derived from three complementary *Terra* instruments: the Clouds and the Earth's Radiant Energy System (CERES), the Multiangle Imaging Spectroradiometer (MISR), and the Moderate Resolution Imaging Spectroradiometer (MODIS). CERES, MISR, and MODIS are being used to investigate the critical role aerosols play in modulating the radiative heat budget of the earth–atmosphere system. CLAMS' primary objectives are to improve understanding of atmospheric aerosols, to validate and improve the satellite data products, and to test new instruments and measurement concepts. A variety of in situ sampling devices and passive remote sensing instruments were flown on six aircraft to characterize the state of the atmosphere, the composition of atmospheric aerosols, and the associated surface and atmospheric radiation parameters over the U.S. eastern seaboard. Aerosol particulate matter was measured at two ground stations established at Wallops Island, Virginia, and the Chesapeake Lighthouse, the site of an ongoing CERES Ocean Validation Experiment (COVE) where well-calibrated radiative fluxes and Aerosol Robotic Network (AERONET) aerosol properties have been measured since 1999. Nine coordinated aircraft missions and numerous additional sorties were flown under a variety of atmospheric conditions and aerosol loadings. On one "golden day" (17 July 2001), under moderately polluted conditions with midvisible optical depths near 0.5, all six aircraft flew coordinated patterns vertically stacked between 100 and 65 000 ft over the COVE site as *Terra* flew overhead. This overview presents a description of CLAMS objectives, measurements, and sampling strategies. Key results, reported in greater detail in the collection of papers found in this special issue, are also summarized.

1. Introduction

It is well recognized that the environment of the earth–atmosphere system is under an unprecedented anthropogenic transformation. Brought on by more than a factor of 5 increase in human population (U.S. Bureau of the Census 2004) and the subsequent activities of mankind over the last century or so, greenhouse gases and aerosols produced by the combustion of fossil fuels, industrial activities, and land use have altered the atmospheric composition so that it is not the same as it was a century ago (Mann et al. 1999; Crowley 2000; Houghton et al. 2001). The resulting increase in surface temperature over this period is estimated to be between 0.4° to 0.8°C (Houghton et al. 2001). Greenhouse gases warm the earth's surface by reducing the thermal emission of radiation to space; their radiative forcings over the past century are known reasonably well. While aerosols primarily affect the planet "directly" through the scattering and absorption of solar radiation and "indirectly" by modifying cloud properties (Twomey 1977), there is substantial uncertainty regarding the

++ Additional affiliation: Joint Center for Earth Systems Technology, University of Maryland, Baltimore County, Baltimore, Maryland.

Corresponding author address: William L. Smith Jr., MS 420, NASA Langley Research Center, Hampton, VA 23681.
E-mail: william.l.smith@nasa.gov

magnitude and spatial distribution of aerosol radiative forcing.

To better understand and quantify aerosol effects, a variety of field campaigns have been conducted recently to characterize aerosol physical and chemical properties and processes. These include the Aerosol Characterization Experiments (ACE-1, -2, and -Asia), the Tropospheric Aerosol Radiative Forcing Observational Experiment (TARFOX), the Sulfate Clouds and Radiation-A (SCAR-A) experiment, the Smoke Clouds and Radiation-B (SCAR-B) experiment, the Indian Ocean Experiment (INDOEX), and the Southern Africa Regional Science Initiative (SAFARI-2000). ACE-1 took place south of Australia in November–December 1995 and measured properties of the natural aerosol in the remote marine boundary layer (Bates et al. 1998). SCAR-A and TARFOX (Russell et al. 1999), designed to measure and analyze aerosol properties and effects along the U.S. eastern seaboard, took place during the summers of 1993 and 1996, respectively. ACE-2 took place in the North Atlantic Ocean in June–July 1997 and focused on the radiative effects and processes controlling anthropogenic aerosols from Europe and desert dust from Africa as they were transported over the North Atlantic Ocean (Raes et al. 2000). The goal of SAFARI-2000 is to understand the key linkages between the physical, chemical, and biological processes, including human activities, that compose the southern African biogeophysical system (Swap et al. 2002). ACE-Asia took place during the spring of 2001 off the coast of China, Japan, and Korea (Huebert et al. 2003). This region includes many types of aerosol particles of widely varying composition and sizes derived from one of the largest aerosol source regions on earth. ACE-Asia made several important measurements of wind-blown dust, urban pollution, and marine aerosols.

Satellites, which offer a global perspective with high spatial and temporal resolution, have become important tools for measuring the changing characteristics of the earth's atmosphere and the associated radiative heat fluxes that define the climate. Improvements in satellite sensor technologies and constituent retrieval techniques have helped to advance our understanding of the climate system. However, the reliable prediction of anthropogenic effects on climate remains elusive, because 1) anthropogenic forcings have not been adequately quantified, and 2) feedbacks between important climate processes are poorly understood and thus questionably represented in climate models (Houghton et al. 2001). The feedback in a climate model can be tested confidently, only if the forcing over the test interval is known. The National Aeronautics and Space Administration (NASA) is responding to this shortcoming with an Earth Observing System (EOS) consisting of a series of satellites configured with advanced imagers and sounders to quantify the physical and radiative properties of aerosols, clouds, trace gases, and surface properties while simultaneously measuring the earth's energy budget. This synergistic view of the earth and its atmosphere from space offers unprecedented information to test and improve climate models, vital tools necessary not only for an improved understanding of the climate system but for improved prediction and mitigation of global change. Since the success of this approach will depend on the accuracy and representativeness of the satellite products, an important aspect of the EOS is the validation of these products and subsequent improvements in the techniques and algorithms used to derive them.

The Chesapeake Lighthouse and Aircraft Measurements for Satellites (CLAMS) field experiment was designed to partially address this need. CLAMS, specifically designed to assess satellite-derived aerosol products and radiative effects, was conducted from 10 July to 2 August 2001 from the NASA Wallops Flight Facility (WFF) on Wallops Island, Virginia. This location, which offers access to one of the world's major plumes of urban and industrial haze as it moves from the eastern continental United States over the Atlantic Ocean, was sampled extensively during SCAR-A in 1993 and TARFOX in 1996. Most of the participating aircraft in CLAMS were based at the WFF. The site is also in close proximity to several Aerosol Robotic Network (AERONET) stations, an ocean-based surface remote sensing site at the Chesapeake Lighthouse, several National Oceanic and Atmospheric Administration (NOAA) ocean buoys, and other surface sites.

The Clouds and the Earth's Radiant Energy System (CERES), Multiangle Imaging Spectroradiometer (MISR), and the Moderate Resolution Imaging Spectroradiometer (MODIS) are three instruments on the first EOS satellite (*Terra*, launched in December 1999) being used to investigate the critical role aerosols play in modulating the earth's radiation budget. CLAMS' main focus is on assessing and improving the new data products being derived from these instruments to increase our knowledge and reduce uncertainties associated with atmospheric aerosols and their radiative impacts. While focused, regional field campaigns such as CLAMS do not provide the statistical sampling necessary for a true global validation of satellite products; they do play a critical role in testing and improving the satellite algorithms because of the unusually complete datasets that are obtained to characterize properties of the atmosphere and surface. Furthermore, the measurements provide details about aerosols, such as particular height-resolved aerosol radiative and microphysical properties, some of which cannot be retrieved from any current or anticipated satellite data; these data are a test bed for current aerosol and chemical transport models.

Figure 1 schematically depicts many of the key platforms and the primary measurements made during CLAMS. Details regarding CLAMS objectives, plat-

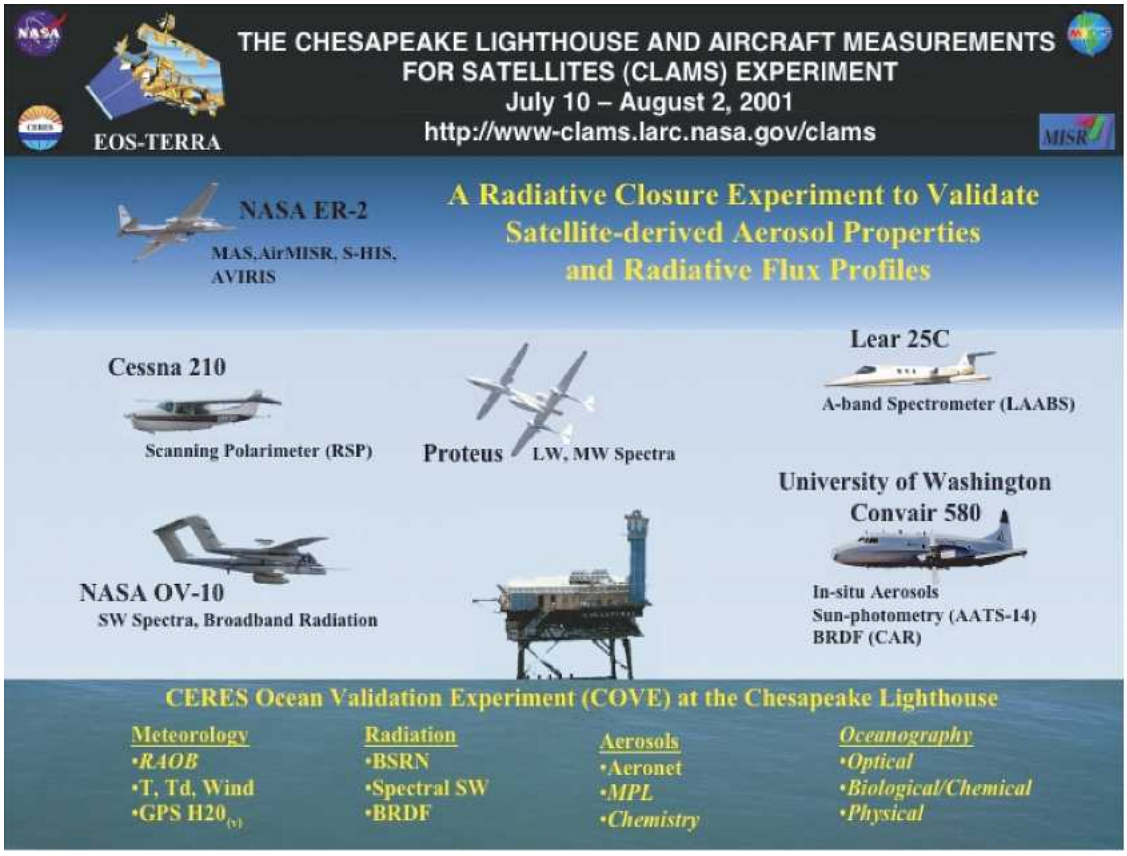

FIG. 1. Schematic depiction of CLAMS platforms and measurements.

forms, instrumentation, measurement strategy, and a summary of early results are given below.

2. CLAMS objectives

CLAMS was designed to provide the verification data needed to properly assess satellite retrievals of a variety of geophysical parameters but is primarily focused on improving our knowledge and reducing uncertainties associated with atmospheric aerosols and their radiative impacts. The approach was to characterize the atmosphere and surface in as much detail as possible using an array of surface-based remote sensing stations and instrumented aircraft. CLAMS is one of the first aerosol experiments conducted after *Terra* became operational in late February 2000 and emphasizes the new data products being derived from CERES, MISR, and MODIS. Associated with this overall goal are a number of contributory objectives:

1) Utilize aircraft and surface-based observations of aerosols and radiation to validate satellite aerosol retrievals over land and ocean through sensor-to-sensor intercomparisons, and to test key assumptions regarding the aerosol forward models, the surface boundary conditions, spatial variability, and the presence of thin cirrus.
2) Perform a variety of closure studies to test the mutual consistency of measurements and calculations of aerosol properties and effects, radiative properties, particularly the ocean bidirectional reflectance distribution function (BRDF), and ultimately broadband shortwave surface and top-of-atmosphere (TOA) radiative fluxes to assess and reduce uncertainties in radiative forcing estimates.
3) Perform aircraft experiments to aid in the development of aerosol optical thickness and absorption retrievals over sun glint.
4) Assess the quality of radiation and aerosol measurements made at the Chesapeake Lighthouse as part of a long-term satellite validation campaign.
5) Test the cloud-screening procedure for the MODIS aerosol algorithm and evaluation of MODIS water vapor retrievals.

During CLAMS, measurements were also acquired from several aircraft instruments flown to evaluate retrieval algorithms for planned sensors (i.e., Earth Observing Scanning Polarimeter (EOSP), Geosynchronous Imaging Fourier Transform Spectrometer (GIFTS) and for those proposed (Oxygen A-band spec-

trometer) for future satellite platforms. These efforts not only benefited from the wide range of correlative data obtained during CLAMS but also contributed to the overall science objectives of CLAMS.

3. CLAMS platforms and measurements

a. Terra satellite

The *Terra* satellite carries a payload of five remote sensors that, together, are making comprehensive measurements of the state of earth's environment and ongoing changes in its climate system. *Terra* is in polar orbit with a local equator crossing time at about 10:30 A.M. Data products derived from three of these sensors (CERES, MISR, and MODIS) are the primary focus of CLAMS and are briefly described here.

CERES has three detectors to measure radiation at a nominal spatial resolution of 20 km in the 8–12-μm "window," the shortwave (0.2–5.0 μm), and the total (0.2–100 μm) broadband, and extends previous measurements of the earth's radiation budget dating back to 1979 (Wielicki et al. 1996). CERES' unprecedented calibration and angular and spatial sampling of key systematic radiative flux variables provide critical and widely used data for testing the ability of climate models to predict the climatic impact of clouds and aerosols. CERES data have recently been used to reveal radiation budget anomalies that exceed climate model predictions by a factor of 2 to 4 (Wielicki et al. 2002). CERES data products include, arguably, the most accurate and rigorous surface and atmosphere global radiative fluxes ever produced for the earth's climate system. This is accomplished by combining radiative transfer calculations with cloud properties derived from MODIS, model analyses of atmospheric state, and the MATCH chemical transport model (Collins et al. 2001) assimilated MODIS aerosol information. This procedure is partially constrained by the CERES TOA fluxes, permitting the global simulation of explicit forcings of clouds and aerosols. Charlock et al. (2004) describe this effort in more detail and present an assessment of its accuracy using CLAMS data.

An important aspect of CERES is that the spacecraft is deployed with two identical instruments that permit data to be collected in two scanning modes simultaneously. The primary data-collection mode utilizes an azimuthally fixed scan pattern that scans in elevation, either along track or cross track. A second instrument is programmed to rotate azimuthally while it scans in elevation, as is required to develop the angular distribution models used to invert CERES-measured radiances to fluxes (Loeb et al. 2003). The instrument can also be programmed to lock onto a ground target to enhance data collection for field campaigns or to align the scan plane with that of another satellite sensor for direct comparisons. During CLAMS, one CERES instrument was programmed to lock onto the position of the Chesapeake Lighthouse, which increases the angular sampling domain for testing CERES fluxes with CLAMS data by about a factor of 10. An example of this scan pattern is shown in Fig. 2. (More information on the CERES program and data products can be found online at http://asd-www.larc.nasa.gov/ceres/ASDceres.html.)

The MISR instrument measures upwelling shortwave radiance in 36 channels, four spectral bands centered at 0.446, 0.558, and 0.672 μm, at each of nine view angles spread out in the forward and aft directions along the flight path, at ±70.5°, ±60.0°, ±45.6°, ±26.1°, and nadir (Diner et al. 1998a). Because MISR samples a large range of scattering angles, covering about 60° to 160° in midlatitudes, the data contains information about aerosol size, shape, and single scattering albedo, especially over dark water (Kahn et al. 1998, 2001). It also captures airmass factors ranging from 1 to 3, offering high sensitivity to optically thin aerosol layers and allowing aerosol retrieval algorithms to distinguish top-of-atmosphere reflectance contributions from the surface and atmosphere (Martonchik et al. 1998, 2002).

In CLAMS, the MISR team aimed at collecting detailed aircraft and COVE data characterizing the atmosphere and surface in the study area, coincident with as many as possible of the five MISR overflights during the campaign. The overflights all occurred between 1600 and 1612 UTC, and priority was given to cloud-free conditions. Such data are used to test multiangle aerosol retrieval approaches over dark water, to quantify the contribution of sub-MISR-pixel scene variabil-

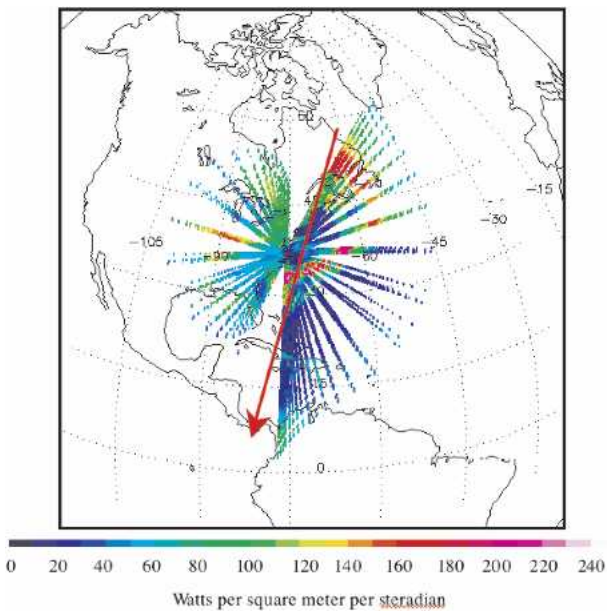

FIG. 2. Example of CERES programmable scan pattern locked onto the Chesapeake Lighthouse that was executed for all *Terra* overpasses during CLAMS resulting in a factor of 10 increase in angular sampling for validation purposes (courtesy of K. Priestley, NASA LaRC).

ity to aerosol measurement uncertainty, and to help assess the MISR instrument's low-light-level calibration. Having MISR data coincident with the aircraft MISR analog, AirMISR (Fig. 3), allows comparisons of multiangle radiances more directly than can be done with nadir-only views that are collected during most field experiments. Low-light-level calibration results are given by Kahn et al. (2005).

MODIS (King et al. 1992, 2003) is another key satellite instrument for describing the spatial and temporal characteristics of global aerosol, cloud, and surface properties. MODIS is a 36-band cross-track imager with variable spatial resolution of 250 m to 1 km. Because of the fine spatial resolution and wide spectral range (0.41 to 14.1 μm), MODIS is paramount in identifying and masking clouds and provides the cloud mask not only for products derived from MODIS reflectances, but also for the CERES products. The MODIS 1.38-μm channel is ideally suited to identify thin cirrus (Gao et al. 2002). Seven bands from 0.47 to 2.13 μm are used to estimate aerosol optical thickness and particle size parameters. In particular, the longer wavelengths (1.24–2.13 μm) are sensitive to aerosol size and permit accurate separation of fine-mode and coarse-mode aerosol over oceans. The MODIS aerosol retrieval and data products are discussed in detail by Remer et al. (2005).

b. GOES-8

The *Geostationary Operational Environmental Satellite-8* (*GOES-8*) imager measures radiances in four channels (3.9, 6.7, 10.8, and 12.0 μm) with a nominal resolution of 4 km and in the visible (0.63 μm) at 1 km. *GOES-8* imager data taken every 15 min during CLAMS experiment days were obtained to support the aircraft operations, and because their high temporal and spatial resolution have proven useful in the analyses of CLAMS data. These data may be found in Man-computer Interactive Data Access System (McIDAS) and Graphics Interchange Format (GIF) in the CLAMS data archive. The GIF imagery is also available on CLAMS' Web page including flight-track overlays for all the aircraft.

c. Surface sites

A number of surface sites were established or augmented to support CLAMS objectives. The most heavily instrumented and the anchor point for many of the aircraft experiments was the Chesapeake Lighthouse located 120 km south of the WFF. This platform is discussed in detail in the next section. Levy et al. (2005) describe other sites including the local land-based AERONET stations, a sun-photometer site at NASA Langley, and a handheld Microtops sun-photometer network. Castanho et al. (2005) describe filter-sampling systems deployed at a site established on Wallops Island and at the lighthouse. The University of Wisconsin deployed a surface-based, upward-looking Atmospheric Emitted Radiance Interferometer (AERI; Smith et al. 1999) on Wallops Island. AERI measures infrared radiation at high spectral resolution from 3 to 25 μm from which vertical profiles of boundary layer

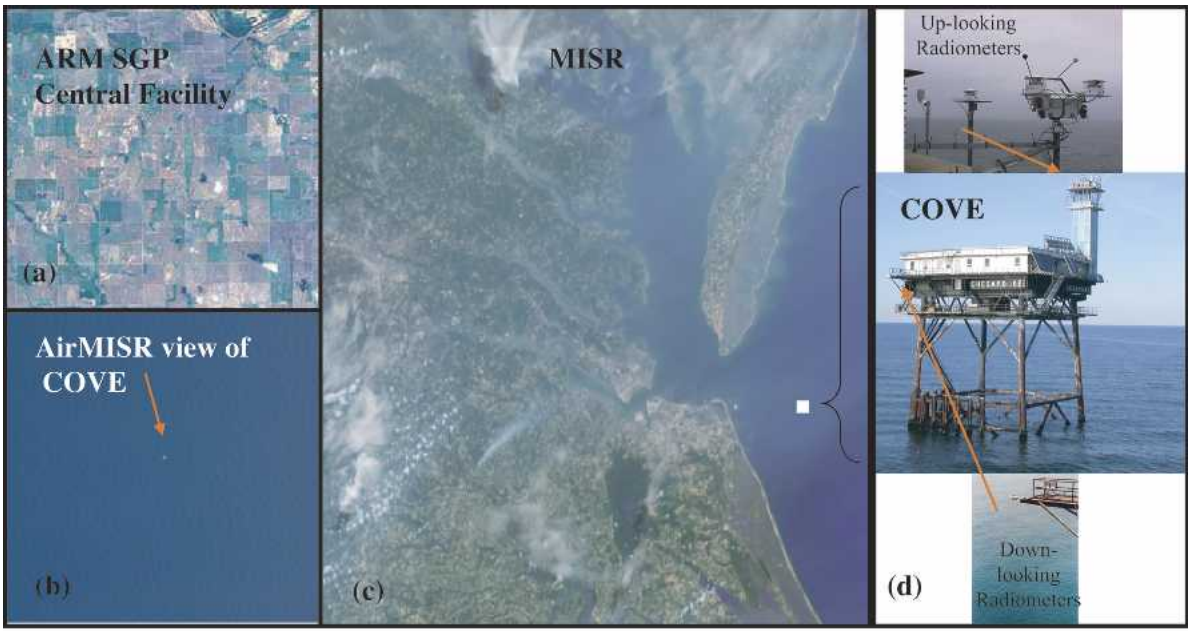

FIG. 3. Multiple views of the COVE site at the (d) Chesapeake Lighthouse from (b) AirMISR and (c) MISR on 17 Jul 2001. The Landsat Thematic Mapper (TM) data (courtesy of http://daac.gsfc.nasa.gov/CAMPAIGN DOCS/SGP99/LC99.html) of the (a) DOE ARM SGP site is shown in contrast to the spatially uniform ocean background surrounding the Chesapeake Lighthouse, illustrating the utility of the COVE site for satellite validation and radiative forcing studies.

temperature and humidity may be derived. Several moored buoys operated by the NOAA National Data Buoy Center (NDBC) were also important targets for aircraft overpasses characterizing the ocean optical properties, an important lower boundary condition for airborne and satellite aerosol remote sensing. The buoy data provide corroborative measurements of the associated wind and wave spectra, which are used to test ocean optics parameterizations. Figure 4 depicts the location of key CLAMS surface sites.

CHESAPEAKE LIGHTHOUSE: A UNIQUE OCEANIC SURFACE SITE

Central to CLAMS' measurement strategy is the U.S. Coast Guard's Chesapeake Lighthouse located 25 km east of coastal southern Virginia and the site of an ongoing CERES Ocean Validation Experiment (COVE). Hereafter, this site is referred to as COVE. Because the rationale for developing this site has not been discussed previously in the literature, we briefly present it here.

Two critical problems in satellite-based retrievals of both aerosols and surface radiative fluxes are separating the effects of the surface and the atmosphere and accounting for their spatial variabilities. This is particularly a problem at short wavelengths over vegetated land surfaces where surface albedo can be very large and can vary significantly on many spatial scales. A typical vegetated surface albedo in the visible is about 0.1, while in the near-infrared values near 0.6 or larger are typical. Nearly all long-term surface-based remote sensing sites are located on land. Because of the heterogeneity of the surrounding land surface, it is unlikely that the surface albedo derived from up- and down-looking radiometers mounted on a tower at these sites can accurately represent the surface albedo even on the scale of a few satellite imager pixels, much less for a 20-km CERES footprint. Furthermore, surface albedo impacts the shortwave radiation budget at the surface via multiple reflections between the ground and the atmosphere. This coupling between radiation and the surface boundary can confound comparisons between modeled and observed SW surface fluxes, including insolation, if the surface albedo is not well known. Li et al. (2002) discuss the impact of this problem for overcast conditions at the Department of Energy (DOE) Atmospheric Radiation Measurement (ARM) Program's central facility (CF) in Oklahoma, one of the world's premier surface remote sensing sites. In clear skies, the impact of uncertainties in surface albedo on computed fluxes is smaller than for overcast conditions, but still comparable to uncertainties in aerosol properties and atmospheric state, and therefore should be considered in direct aesrosol radiative forcing studies. Thus, we have a dilemma in our ability to use land sites for validating CERES shortwave surface fluxes and our ability to reduce radiative forcing uncertainties. CERES is addressing this problem with COVE (Fig. 3), where the ocean provides a uniform background compared to that at most land sites; the albedo is low and well known (Jin et al. 2002). Therefore, the time-averaged upwelling and net radiation measured by radiometers at COVE represent a large area, a unique aspect not found at other surface sites such as the ARM Southern Great Plains (SGP) site shown in Fig. 3a. COVE is well offshore, and instrumentation is deployed 20 to 30 m above the sea surface, well above the most intense sea spray. Nevertheless, an automated spray wash system is activated daily to keep the domed radiometers clean and to protect the integrity of the data.

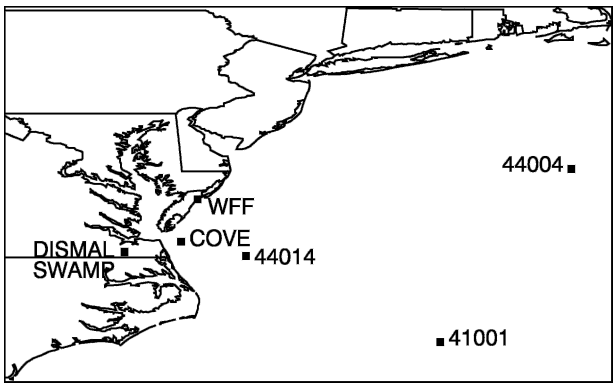

FIG. 4. Map of CLAMS surface sites and key NOAA NDBC buoys.

COVE was established at the Chesapeake Lighthouse in late 1999. Since that time, broadband shortwave (SW; direct and diffuse) and longwave (LW) fluxes, Multifilter Rotating Shadow band Radiometer (MFRSR) SW fluxes, and an AERONET-Cimel sun photometer for spectral radiative and aerosol optical properties (Holben et al. 1998) have been measured and archived. COVE is a participating site in the global Baseline Surface Radiation Network (BSRN) (Ohmura et al. 1998), a project of the World Climate Research Programme (WCRP). Thus, radiation measurements at COVE adhere to the BSRN calibration protocols. A sun glint program is also operated at COVE consisting of a scanning sun photometer (Schulz SP1A) to measure directional upwelling reflectances or BRDF to test and improve ocean optics parameterizations (Su et al. 2002). A meteorological applications of the global positioning system network of defense satellites (GPS-MET) receiver for total column water vapor (Wolfe and Gutman 2000) and a Micro-Pulse Lidar Network (MPLnet) lidar (Welton et al. 2001) are also operational at COVE. Many additional measurements made at COVE during CLAMS are shown in Table 1. Vaisalla radiosondes were launched at 0000 and 1200 UTC daily and during the aircraft operations. The lidar system provided real-time images of the vertical profile of backscatter. The imagery were used to identify altitudes of the aerosol layers to help direct the aircraft and also to document the presence of clouds. A shortwave

TABLE 1. Parameters measured from the COVE site at the Chesapeake Lighthouse during CLAMS.

Parameters	Instrument	Manufacturer	Range (error)
Global shortwave irradiance	Global pyranometer	Eppley, Modified PSP	0.285–2.8 μm (3%–5%)
Global shortwave irradiance	Global pyranometer	Kipp & Zonen, CM31	0.2–4.0 μm (2%)
Direct solar irradiance	Pyrheliometer	Kipp & Zonen, CH1	0.2–4.0 μm (1%)
Longwave irradiance	Pyrgeometer	Eppley, PIR	3.5–50 μm (5%)
Narrowband direct, diffuse, and global solar irradiance	Multifilter rotating shadowband radiometer	Yankee Environmental Systems, MFR-7	0.415, 0.500, 0.615, 0.670, 0.870, 0.936 μm (5%)
Narrowband aerosol optical properties	Sun photometer	CIMEL Electronique, 318NVBS5	0.340, 0.380, 0.440, 0.500, 0.670, 0.870, 1.020 μm (5%)
Directional upwelling radiance	Sun photometer	Schulz, SP1-A	0.45, 0.50, 0.675, 0.872 μm (5%)
Vertically resolved cloud, aerosol properties	Micropulse lidar	Science and Engineering Services	0.523 μm
Spectral shortwave irradiance	Full-range fieldspec	Analytical Spectral Devices	0.35–2.2 μm-10 at nm res. (3%–5%)
Scattering coefficient	Nephelometer	TSI	0.45, 0.55, 0.70 μm (10%)
Absorption coefficient	Aphelometer	Radiance Research PSAP	0.567 μm (25%)
Total CN concentration	Condensation particle counter	TSI	Sizes $>$ 0.07 μm
Aerosol elemental composition, mass concentration	Stacked nucleopore filter unit	Sao Paulo University, Brazil	(4%–8%, 10–50 ng m^{-3})
Directional upwelling radiance	Sun photometer	Schulz, SPI-A	0.45, 0.50, 0.675, 0.872 μm (5%)
T, P, RH, U, V, wave spectra	Standard buoy/meteorological station	NOAA	—
T, P, RH (vertical profiles)	Radiosonde	Vaisalla 80	(0.2°C, 0.5 hPa, 3%)
Columnar water vapor	GPS	NOAA FSL GPSMET	(~2 mm IPW)

spectrometer (Analytical Spectral Devices, Inc.) measured downwelling irradiance from 0.35 to 2.2 μm with 0.01-μm resolution and was modified to periodically view the solar disk through a collimating tube to estimate spectral aerosol optical depth (AOD). Instrumentation was deployed to determine in situ radiative, physical, and chemical characteristics of aerosols found in the lower atmosphere near the surface. Castanho et al. (2005) describe a filter system deployed to determine the chemical composition, mass concentration, and absorption properties, including the equivalent black carbon content of the aerosols. Data from a three-wavelength (0.45, 0.55, and 0.70 μm) nephelometer deployed to measure scattering coefficients and a Particle Soot Absorption Photometer (PSAP) to measure aerosol light absorption at 0.567 μm provide information on the single scattering albedo (SSA) at 0.55 μm. A condensation nuclei (CN) counter was deployed to measure the total concentration of aerosol particles.

A team from the Old Dominion University Center for Coastal Physical Oceanography (http://www.ccpo.odu/~orca) made a suite of oceanographic measurements to support CLAMS closure studies and to satisfy their own validation objectives pertaining to satellite ocean color. Studies reported by Jin et al. (2005) and Chowdhary et al. (2005) demonstrate the utility of this valuable ocean optics data collected during CLAMS.

d. Aircraft

Six research aircraft participated in CLAMS: NASA's ER-2 and OV-10, the University of Washington Convair 580 (CV-580), the *Proteus*, a Cessna 210, and a Lear jet.

The NASA ER-2, serving as a remote sensing validation platform, flew at 65 000 ft with MODIS airborne simulator (MAS; King et al. 1996) and AirMISR (Diner et al. 1998b). The Scanning High-Resolution Interferometer Sounder (S-HIS) and the Advanced Visible/Infrared Imaging Spectrometer (AVIRIS) measured longwave and shortwave spectra, respectively. Typical flight patterns included a series of adjacent legs parallel to the solar plane to test new aerosol retrieval algorithms for sun glint from MAS, daisy patterns for AirMISR BRDF, and single track legs or racetracks parallel to the *Terra* orbit track and centered over one of the surface sites (typically COVE, one of the NOAA buoys, or a land-based target) for sensor intercomparisons, geolocation, or calibration purposes (Table 2). The latter track also provided multiangle measurements of the target area with AirMISR.

The University of Washington Convair 580 was the "workhorse" of CLAMS, instrumented to measure the physical and chemical properties of aerosols in situ. The CV-580's instrument complement included nephelometers, an aphelometer, two forward scattering spectrometer probes (FSSPs) for small and large particles, CN counters, an aerosol spectroreflectometer with a nucleopore filter collection system to measure aerosol absorption, and Teflon and quartz filter collection systems for measuring ionic and carbonaceous species. A complete overview of these instruments along with the flight plans and summaries of each flight can be found at http://cargsun2.atmos.washington.edu, while Magi et al. (2005) discuss the measurements of aerosol properties. The CV-580 also deployed several radiometric instruments to measure spectral and broadband shortwave radiation, including the 14-channel NASA AMES

TABLE 2. CLAMS mission summary: *Terra* overpass, mean AOD, and aircraft flights.

Date (general location)	*Terra* overpass (UTC)	Mean AOD	Aircraft	Takeoff (UTC)	Land (UTC)	Remarks
10 Jul 2001 (COVE vicinity)	1606	0.23	CV-580	1725	2220	BRDF, total AOD survey, slow extinction profile (surface to 12 000 ft), aerosol chemistry at 10 000 and 4000 ft
			Cessna	1745	2205	Rosettes at 200 and 12 000 ft
			OV-10	1815	1920	600-ft survey
			Proteus	1430	1830	Transit from Madison, WI, 55 000-ft mapping over Maryland and Virginia eastern shore, slow profile over Wallops
12 Jul 2001 (COVE vicinity)	1554	0.08	ER-2	1110	1635	Glint experiment, *Terra* track
			Proteus	1133	1639	Profile, buoy 41001 leg at 55 000 ft
			OV-10	1205	1420	600-ft flux survey, 3000- and 6000-ft racetracks
			CV-580	1315	1751	Extinction profile (6000 ft to surface), BRDF, profile (surface to 10 000 ft) aerosol chemistry (6000, 2400, 1500 ft), some smoke at 2400 ft, total AOD survey
14 Jul 2001 (COVE vicinity)	1541	0.08	Cessna	1345	1730	Spiral (2000 to 12 000 ft), 12 000-ft rosettes
			Proteus	1415	1850	Profile, 55 000-ft mapping, Wallops profile
			CV-580	1440	1745	Total AOD survey, profile to 10 000 ft, BRDF, radiosonde observation (raob) chase near Wallops
			OV-10	1555	1730	600-ft survey
17 Jul 2001 (COVE vicinity)	1612	0.47	CV-580	1235	1812	Slow profile to 12 000 ft, aerosol chemistry (9000, 6000, 3000 ft), total AOD survey, BRDF
			ER-2	1300	1701	Glint pattern, AirMISR geolocation pattern, *Terra* track, buoy 44014
			OV-10	1623	1812	10 000 ft, 3000-ft racetrack, 600-ft survey
			Cessna	1330	1800	12 000-ft glint experiment, rosettes at 200 and 12 000 ft, Dismal Swamp tracks
			Proteus	1431	1832	COVE profile, 55 000-ft mapping, Wallops profile
			Lear 25C	1500	1800	40 000-ft *Terra* tracks
23 Jul 2001 (east of Wallops)	1536	0.06	CV-580	1402	1639	BRDF, total AOD survey, profile to 10 000 ft
26 Jul 2001 (COVE)	1606	0.17	OV-10	1316	1504	600- and 100-ft surveys
			Proteus	1430	1830	55 000-ft mapping, buoy 44014
			CV-580	1535	1904	Total AOD survey, slow profile to 10 000 ft, aerosol chemistry at 2200 and 1100 ft, BRDF at buoy 44014, AOD survey
			OV-10	1622	1830	600-ft survey
30 Jul 2001 (COVE)	1541	0.06	CV-580	1617	1946	Lots of clouds: AOD survey, BRDF, 10 000-ft profile, AOD run, cloud structure measurements at 5500 ft, BRDF
			ER-2	1628	1948	Glint pattern, *Terra* track
			OV-10	1420	1640	100- and 600-ft surveys beneath overcast, 3500-ft daisy above cloud deck
31 Jul 2001 (COVE, 44004, (Dismal Swamp)	1624	0.08	ER-2	1259	1857	AirMISR star patter over buoy 44004, COVE tracks, AirMISR geolocation pattern
			CV-580	1433	1956	AOD survey, BRDF over dark water (buoy 44004), profile to 10 000 ft, Dismal Swamp BRDF
			Lear	1520	1807	40 000-ft tracks to 44004
			OV-10	1607	1806	COVE 100- and 600-ft surveys
			OV-10	1957	2140	Dismal Swamp daisy pattern
2 Aug 2001 (COVE vicinity)	1612	0.1	ER-2	1459	Dryden	*Terra* track, AirMISR geolocation pattern, return to NASA Dryden
			CV-580	1530	2037	6000-ft radiometer comparison with OV-10, AOD survey, profile to 10 000 ft, aerosol chemistry (2900 ft), land Norfolk (CAR door stuck), profile to 10 000 ft, BRDF
			OV-10	1530	1743	Radiometer comparison with CV-580, flux profile to 3000 ft, 100-ft survey
			OV-10	1957	2140	100- and 600-ft surveys

Airborne Tracking Sunphotometer (AATS-14) (Redemann et al. 2005) and the NASA Goddard Cloud Absorption Radiometer (CAR; King et al. 1986). The AATS-14 provided continuous measurements of aerosol optical depth, while the CAR provided the important lower boundary condition (BRDF) (Gatebe et al. 2005), both critical for radiative closure studies and validation of AOD derived from *Terra* and ER-2 airborne data. Although the CAR measurements are limited to the wind and sea conditions and solar geometries encountered during CLAMS, they will be useful for checking the validity of the long-term measure-

ments of ocean BRDF being made at COVE under a much wider range of conditions (Su et al. 2002).

The typical flight scenario for the CV-580 included BRDF patterns near the beginning and end of each mission, a 30-min leg flown at 100 ft centered at satellite overpass time to characterize the total column AOD with the AATS-14, and a detailed characterization of two to four aerosol layers. Each layer was sampled for up to 45 min to ensure sufficient aerosol mass was collected on the filters. Along-wind and cross-wind legs were flown to capture the horizontal variabilities. A quick ascent from the surface to 12 000 ft prior to the detailed aerosol characterization provided the flight scientist the information needed to determine what altitude and how many layers to characterize and also to provide an AOD profile for closure studies.

A third key aircraft for CLAMS was the NASA Langley Research Center (LaRC) OV-10 configured to measure upwelling and downwelling longwave (broadband) and shortwave (broadband and spectral) irradiances. The broadband instruments are manufactured by Eppley Laboratories, Inc. The spectral shortwave measurements are obtained with Analytical Spectral Devices Full Range (ASD-FR) spectrometers, which measured irradiance from 0.35 to 2.20 μm at about 0.01-μm resolution (Kindel et al. 2001). The primary objectives of the OV-10 were to conduct low-altitude (100 and 600 ft) surveys of spectral and broadband fluxes to measure the spatial variability of ocean optics on various scales to help understand platform effects on the measurements of upwelling radiation at COVE, to determine how well COVE measurements represent the sea in general, and to determine the shortwave flux profile below 10 000 ft.

Three additional aircraft participated in CLAMS. The *Proteus*, owned by Scaled Composites, Inc., flew a payload that included the National Polar-Orbiting Operational Environmental Satellite System (NPOESS) Airborne Sounding Test Bed—Interferometer (NAST-I), NAST-M (a microwave radiometer component of NAST), and the Far IR Sensor for Cirrus (FIRSC). NAST-I is a scanning interferometer measuring high-resolution (0.25 cm^{-1}) spectra from 3.7 to 15.4 μm to map sea surface temperature (SST) and atmospheric profiles of temperature, water vapor, and trace gases (Smith et al. 2005). Most of the *Proteus* flight hours were spent mapping at 55 000 ft, but at times the *Proteus* conducted slow ascending and descending spirals over Wallops and COVE between 55 000 ft and close to the surface. A nine-channel visible and near-infrared Research Scanning Polarimeter (RSP) was flown on a Cessna 210. The Cessna 210 participated in CLAMS from 10 to 22 July, making intensity and polarization measurements to retrieve aerosol and ocean optical properties (Chowdhary et al. 2005). Finally, a new NASA Langley Airborne A-Band (0.765 nm) Spectrometer (LAABS) was flown for the first time during CLAMS on a Lear jet at 40 000 ft to demonstrate its capability for aerosol optical thickness retrievals (M. Pitts 2001, personal communication).

4. Experiment summary and key results

During CLAMS, coincident observations of atmospheric state parameters, radiation, ocean optics, and aerosol properties were obtained to satisfy CLAMS objectives. Table 2 lists the key aircraft, flight profiles, *Terra* overpass information, and mean midvisible AOD for each of the nine experiment days. Figure 5 shows an altitude time line for the aircraft operations conducted over COVE on 17 July 2001. This flight scenario is typical of CLAMS aircraft operations, although not all aircraft participated in every flight, the target area was sometimes moved to include offshore buoys or adjacent cloud-free areas, and the timing of some of the profiles was altered for various reasons, mainly cloud avoidance. The aircraft operations were tightly coordinated to maximize the temporal and spatial coincidence of the measurements for future closure studies. The most impressive example of this is demonstrated for CLAMS' "golden day" on 17 July when all six aircraft conducted sampling patterns near COVE and were vertically stacked above COVE near the time of the *Terra* overpass.

Figure 6 depicts a few examples of data collected 17 July. Thirty-minute flight-track segments centered at *Terra* overpass time for each of the aircraft are shown in Fig. 6a with a 1615 UTC *GOES-8* visible image in the background. The region was under mostly cloud-free conditions, with a significant pollution layer with midvisible AOD ranging between 0.4 and 0.5. The range

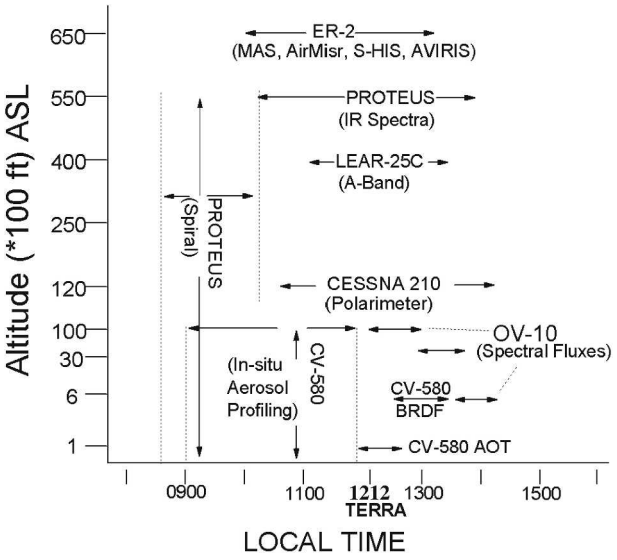

FIG. 5. An altitude time line of CLAMS aircraft depicting typical sampling strategy and the one executed on 17 Jul 2001. The *Terra* overpass occurred at 1212 UTC local daylight time.

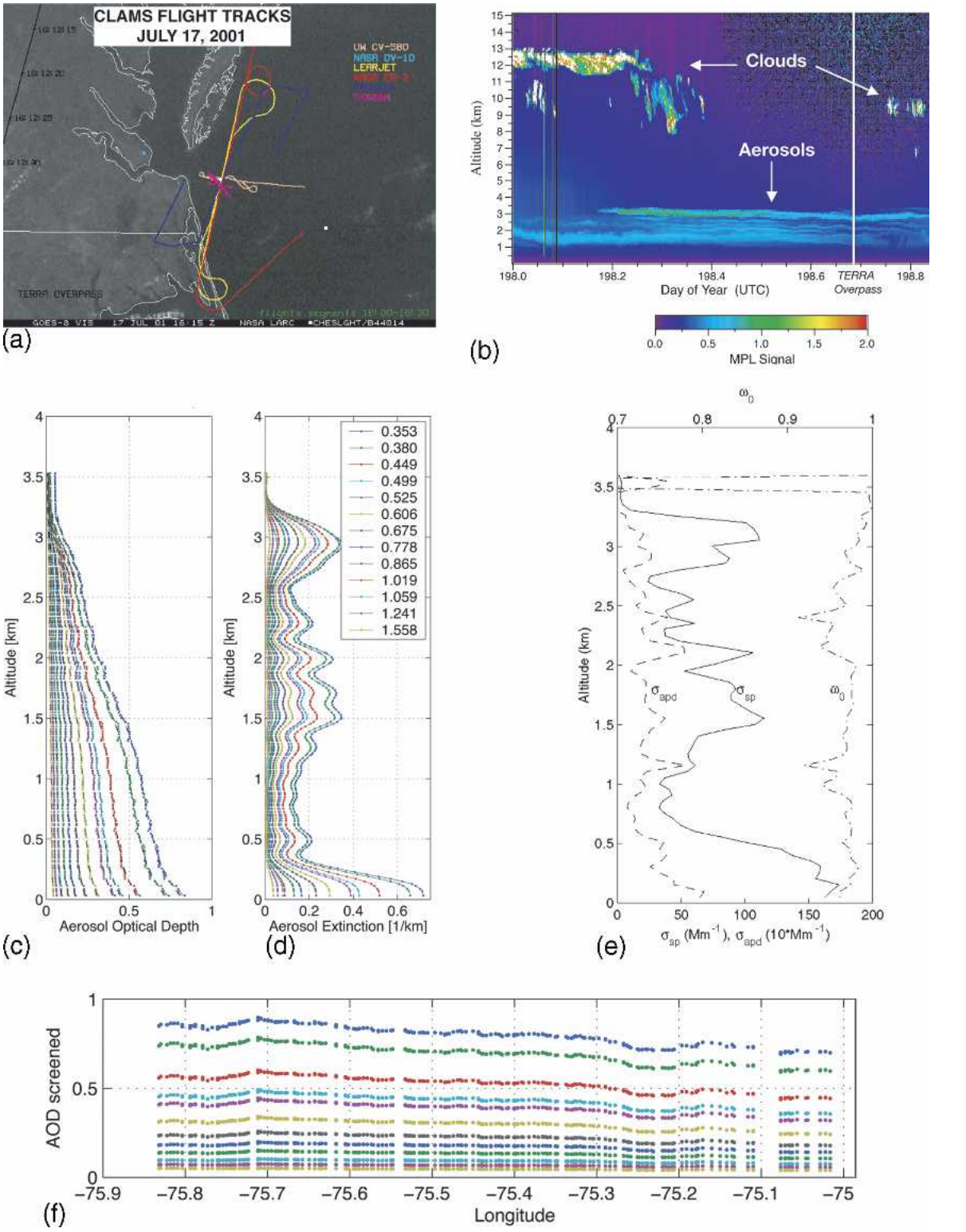

FIG. 6. Examples of data collected for CLAMS closure studies on 17 Jul 2001. (a) The 30-min flight-track segments centered at *Terra* overpass time. (b) Range-corrected and energy-normalized raw signal from the MPL from 0000 to 2359 UTC 17 Jul 2001 (courtesy of J. Welton, NASA GSFC). Vertical profile of (c) spectral aerosol optical depth and (d) extinction derived from AATS-14. (e) Vertical profile of aerosol scattering coefficient (σ_{sp}), dry light absorption coefficient (σ_{apd}), and single scattering albedo (ω_0) derived from CV-580 in situ measurements. Note the legend for (c) and (e) is shown in (d). (f) Horizontal variability in spectral AOD measured byAATS-14 on the CV-580.

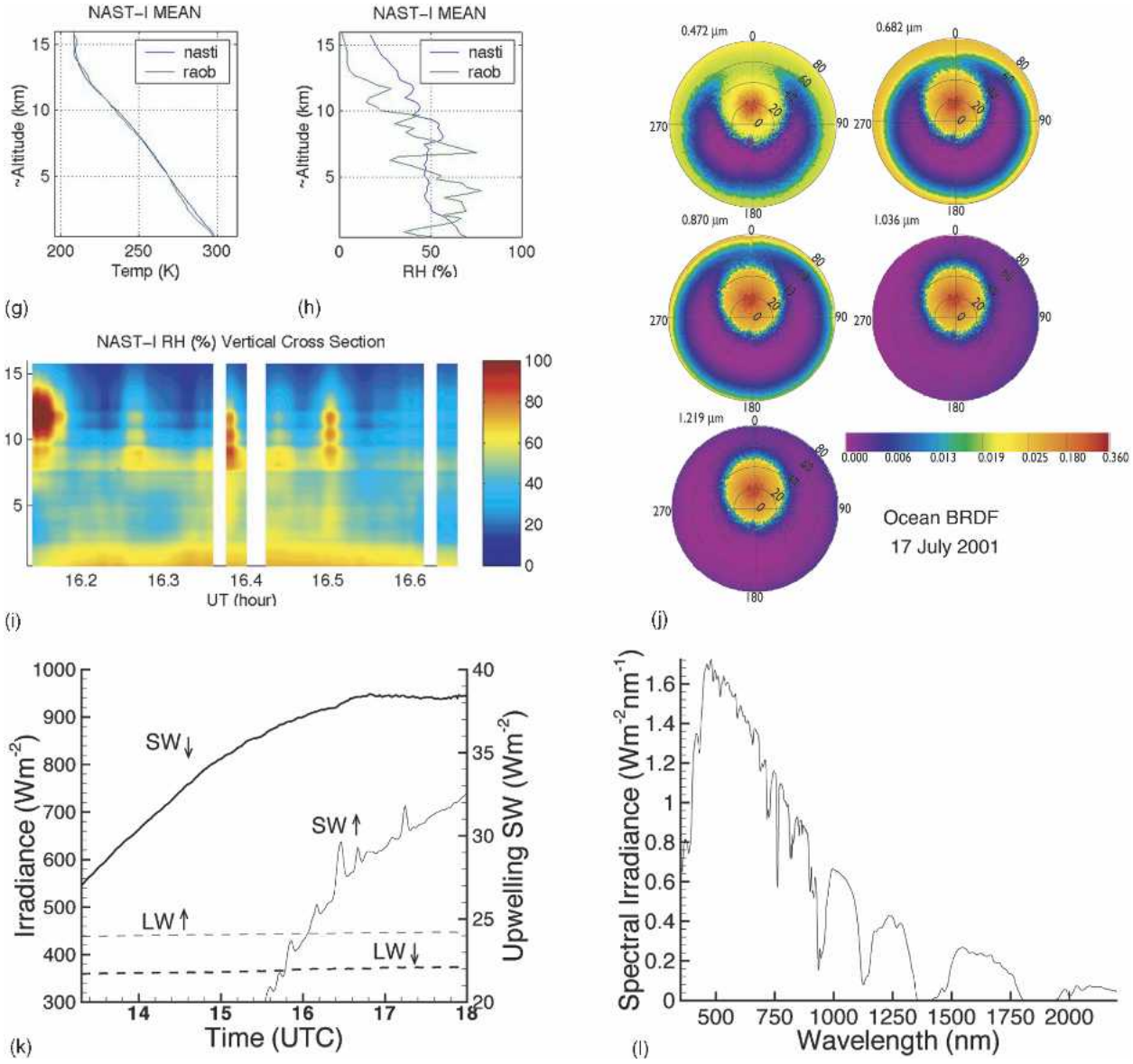

FIG. 6. (*Continued*) (g) Temperature profiles, (h) humidity profiles, and (i) humidity cross sections, derived from NAST-I on *Proteus*. (j) Spectral ocean BRDF derived from airborne CAR aboard the CV-580. (k) Broadband SW and LW fluxes measured at COVE. (l) Downwelling spectral SW flux measured at COVE.

corrected and energy normalized raw MPL signal is shown in Fig. 6b illustrating the complicated vertical stratification of aerosols on this day. The time of the *Terra* overpass at 1612 UTC is marked in the image. A calibration glitch prevented application of appropriate corrections to resolve the lowest 600 m of the aerosol profile from the raw lidar data. Figures 6c–e show the corresponding vertical profiles of aerosol radiative properties obtained from the CV-580 aircraft and resolve the marine layer below 300 m. The vertical profile of column spectral AOD derived from the AATS-14, an airborne sun photometer (Redemann et al. 2005), is shown in Fig. 6c and decreases monotonically with increasing altitude. The spectral channels (in micrometers) are depicted in the legend in Fig. 6d, which shows the corresponding aerosol extinction coefficient derived from the sun-photometer AOD profile. A vertical profile from airborne in situ measurements of the ambient aerosol light scattering coefficient (σ_{sp}), the dry light absorption coefficient (σ_{apd}), and single scattering albedo (ω_0) (Magi et al. 2005) is shown in Fig. 6e. The complex vertical structure in aerosol radiative properties resolved by the in situ sensors corresponds well with the sun-photometer and lidar data, which all show significant scattering layers near 200, 1500, and 3000 m, with less significant layers in between.

Figure 6f shows spectral AOD derived from the sun photometer as the CV-580 made a 75-km transit at an altitude 100 ft above the ocean surface. Over this distance, the horizontal variability is seen to be on the order of 25%, which has implications regarding the appropriate use of ground-based and aircraft measurements of AOD for satellite validation and comparisons to aerosol transport models (Redemann et al. 2005).

Figures 6g–i depict temperature and relative humidity (RH) profiles derived from NAST-I (Smith et al. 2005) onboard the *Proteus*. Flight-leg mean profiles are shown in Figs. 6g and 6h compared to data taken from a radiosonde launched from COVE at 1545 UTC. Smith et al. (2005) show that temperature and RH profiles derived from NAST-I agree with radiosonde data to within 1 K and 15%, respectively. Quantifying the uncertainty in the NAST-I RH retrievals using radiosonde data is complicated by the natural variability of water vapor over small spatial scales. This is evident in the vertical cross section shown in Fig. 6i. The high values of RH found in the beginning of the flight leg between 9 and 14 km appear to be associated with a small area of cirrus over northeast North Carolina that appears in *GOES-8* infrared imagery (not shown). However, the transit between about 16.2 to 16.6 UTC is flown over a cloud-free area. The blips in RH indicate real variability in atmospheric moisture due to convection but not associated with clouds (W. L. Smith Sr. 2004, personal communication).

The spectral BRDF derived from CAR measurements is shown in Fig. 6g. The observed reflectance patterns show peak values of sun glint near the specular direction. Gatebe et al. (2005) compare these observations, under a variety of wind conditions, to traditional model simulations. Spectral and broadband radiative fluxes measured from COVE are shown in Figs. 6h and 6i. The time series of radiative fluxes shown in Fig. 6h is smooth, owing to the cloud-free sky conditions that occurred on this day. The occasional presence of fishing boats near the platform is the likely cause of the small spikes (1–2 W m^{-2}) in upwelling SW flux. Many other measurements were made on this "golden day" and others and are reported in many of the papers in this special issue. We summarize some of the key findings below with reference to more detailed descriptions.

Weather conditions during CLAMS proved to be atypical for July along the mid-Atlantic eastern seaboard. The area experienced an unusual number of cold-frontal passages bringing with them a deep northeasterly flow of cool, clean air. The impact of this unexpected weather pattern on the pollution observed during CLAMS is illustrated in Figs. 7 and 8. Figure 7 depicts the monthly mean 0.50-μm AOD measured by AERONET at COVE in July for the years 2000 to 2003. The AOD of 0.27 in July 2001 is considerably lower than the mean AOD of 0.42 for all four years and less than one-half the 0.57 value observed in July 2002. Forty-eight-hour back trajectories ending 700 m above COVE at solar noon on the nine primary experiment days were computed from the NOAA Air Resources Hybrid Single-Particle Lagrangian Integrated Trajectory (HYSPLIT4) analysis tool (http://www.arl.noaa.gov/ready/hysplit4.html). The results shown in Fig. 8 indicate a significant maritime influence on the experiment area. The most polluted three days, 10, 17, and 26 July, experienced flow out of the west and southwest, where the most significant pollution sources affecting the southeastern Virginia seaboard are located. TARFOX, which was conducted in 1996, encountered more typical July conditions. Magi et al. (2005) compared CLAMS and TARFOX airborne measurements of pollution and found about one-half as many accumulation-mode particles, considerably less optical depth, and higher SSA (less absorbing aerosols) during the CLAMS period. They also found that the relative contributions of sulfate and carbon to the AOD flip-flopped between these two experiments, with carbonaceous species dominating in TARFOX and sulfates dominating in CLAMS. These comparisons suggest that the aerosol properties over the U.S. east coast are

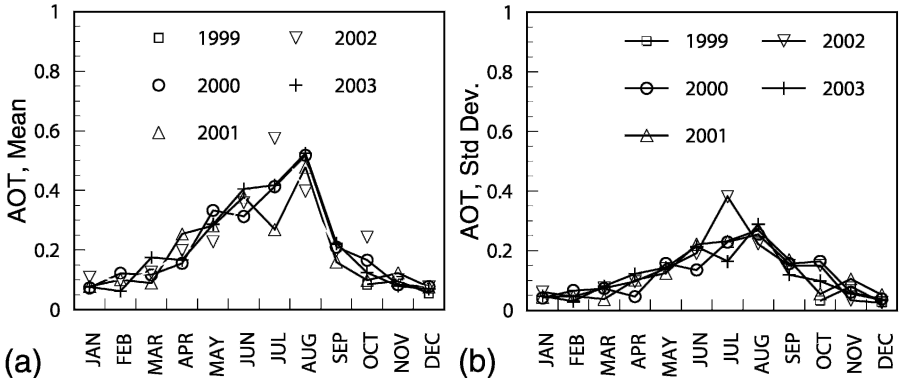

FIG. 7. (a) Mean and (b) std dev of monthly 0.5-μm AOT measured by AERONET at COVE from Oct 1999 through Dec 2003 showing summer peak in AOD and relatively low value during CLAMS in Jul 2001.

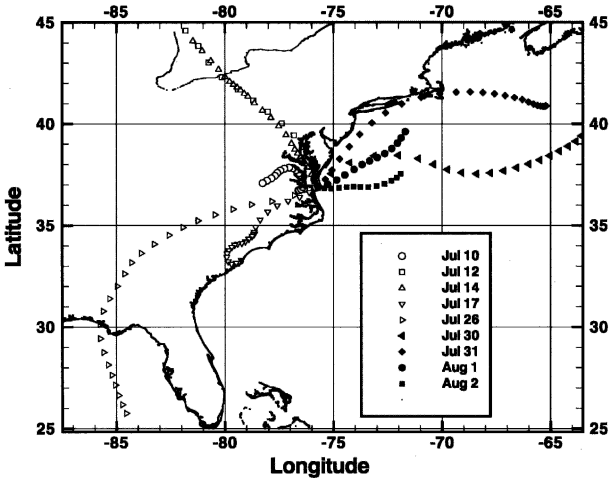

FIG. 8. The 48-h back trajectories ending at solar noon, 700 m above the Chesapeake Lighthouse on CLAMS nine primary experiment days (from NOAA Air Resources Laboratory Hysplit4).

highly dependent on airflow trajectories. The relative importance of water condensed on the aerosols was found to be similar for both experiments. Castanho et al. (2005) determined the main sources of fine- and coarse-mode particles from filter measurements made from aircraft and from the surface sites. They found consistent features in these data, including capture of two long-range transport episodes. On 17 July, a large increase in sulfate concentration was measured owing to an enhancement of regional pollution transported from the eastern United States. During 24 to 26 July, a significant increase in soil dust was observed. Back trajectories for these days support the long-range transport of Saharan dust as a likely source.

Comparisons have been made between *Terra*-derived (MODIS and MISR) aerosol properties and those derived from aircraft and ground-based sun-photometer data obtained during CLAMS. CLAMS is the first field experiment to include multiple sun-photometer measurements made at wavelengths beyond 1 μm including 2.13 μm to validate the full wavelength domain of MODIS aerosol retrievals over ocean. Regarding comparison of the MODIS retrievals, Levy et al. (2005) found agreement to be within the expected uncertainties over oceans (see also Redemann et al. 2005) at all wavelengths but found significant discrepancies over land, particularly in the blue channel. Their analyses suggest that resolving errors in the description of the land surface spectral albedo and applying a more representative urban/industrial aerosol characterization in the MODIS retrieval scheme produces much better agreement with CLAMS verification data. Redemann et al. (2005) found MISR AOD to be systematically larger (by 0.05–0.06) than AATS-14 measurements, but they found good correlation ($r^2 \approx 0.94$) with no spectral dependence. Since the release of the MISR aerosol product used in Redemann et al. (2005), most or all of the discrepancy in the two AOD measurements has been traced to the MISR low-light-level calibration (Kahn et al. 2005). Because of the systematic nature of the difference, coupled with the high correlation, it is expected that the application of the newly developed calibration to the MISR radiances collected in CLAMS will bring the two sets of AOD measurements into very tight agreement. The results further indicate that a lack of small, spherical nonabsorbing particles in an earlier version of the MISR standard aerosol retrieval algorithm, which made the spectral slope of the MISR results too shallow (Schmid et al. 2003), has been corrected.

Redemann et al. (2005) assessed the spatial variability of AOD with AATS-14 data on scales up to 100 km to examine the potential impact of the averaging assumptions used when comparing the satellite retrievals to point measurements (i.e., AERONET AOD). They found typical AOD variations to be 25%–30% over 50-km scales but noted a 60%–70% variation on one day. For one-third of the cases examined at 17- and 50-km scales, the large-scale means differed significantly from the center value, which will contribute to the scatter in satellite and ground-based sun-photometer AOD comparisons. More work is needed to optimize the temporal and spatial averaging procedures used when making such comparisons. Certainly, this points to the utility of global long-term measurements, such as those provided by AERONET, to obtain the statistical sampling necessary to validate satellite retrievals of aerosols (e.g., Remer et al. 2005) and other parameters.

Charlock et al. (2004) report an initial radiative closure experiment, comparing computed SW at the surface to measurements made at COVE and to CERES at TOA. The computations are performed in all-sky conditions with broadband Fu–Liou radiative transfer calculations using cloud properties derived from MODIS and permutations of aerosol properties from MODIS, CLAMS, and the MATCH assimilation. In these calculations, the ocean spectral albedo is prescribed using a lookup table based on results from a coupled ocean–atmosphere radiative transfer model. Complementary spectral model comparisons with aircraft and surface measurements obtained during CLAMS are described by Jin et al. (2005). Despite having to contend with more than typical amounts of sun glint due to the sun–platform–satellite geometry that presented itself during the CLAMS time period, Charlock et al. (2004) report negligible biases for clear-sky insolation throughout the day, in the clearest conditions with low AOD. When clouds were present, they were sometimes confused with sun glint, yielding substantial biases at TOA. Agreement of the direct beam was facilitated by the GPS precipitable water measurements at COVE, while the diffuse component agreement was

good within the bounds of the measurement accuracy of aerosol optical properties. On one day (17 July 2001), during cloud-free conditions with high loading of moderately absorbing aerosols, a calculation using AERONET spectral AOD, asymmetry factor, and single scattering albedo [level 2.0 AERONET with the Dubovik and King (2000) inversion] yielded a diffuse insolation of ~20 W m^{-2} less than that measured. Calculations using single scattering albedo values based on quantities inferred from the MATCH model indicated less absorption: a bias of ~10 W m^{-2} of opposite sign. Flux closure with absorbing aerosols remains a topic requiring further investigation.

Gatebe et al. (2005) developed a rigorous iterative atmospheric correction algorithm that retrieves wind speed and the ocean BRDF (sun glint and water-leaving radiance) simultaneously from the CAR measurements, thus providing a test of commonly used ocean optics models. Results indicate that the Cox–Monk model describes the glint pattern quite well on average but underestimates the center of the glint reflectance by about 30% at low wind speeds (<2–3 m s^{-1}). At high wind speeds, the Cox–Monk model with Gram–Charlier expansion provided the best agreement with the observations.

Chowdhary et al. (2005) performed an evaluation of aerosol retrievals from a scanning multispectral polarimeter. They retrieved a single scattering albedo of 0.91 ± 0.03 for 17 July, for which the lower bound supports that derived from AERONET while the upper bound supports the value derived from the in situ aircraft measurements reported by Magi et al. (2005). They also found good agreement in the accumulation-mode effective radius and spectral AOD when compared to values derived from the aircraft and surface-based sunphotometer data. This important validation effort with the airborne polarimeter is relevant to the development of models to derive aerosol absorption from satellite remote sensing (e.g., Kaufman et al. 2002).

5. Concluding remarks

CLAMS employed a multiplatform approach, with state-of-the-art instrumentation deployed on surface, airborne, and satellite platforms, to provide a comprehensive description of the ocean and atmosphere thermodynamic state, particulate composition, and radiative properties. This integrated dataset is being used to test and improve satellite remote sensing techniques. Results of the analyses performed to date, which have been summarized in this paper and are reported in more detail in this special issue and elsewhere, constitute an important step toward an improved understanding of aerosols and their radiative impacts. CLAMS' rich dataset is available to the scientific community at the NASA Langley Atmospheric Sciences Data Center (ASDC; and can be accessed online at http://eosweb.larc.nasa.gov or through the CLAMS home page at http://www-clams.larc.nasa.gov).

Acknowledgments. CLAMS was sponsored by NASA's Radiation Sciences Program; the CERES, MISR, and MODIS projects; and the EOS Project Science Office. We thank CLAMS flight operations manager, Carl Purgold, for his efforts in the logistical and operational planning of CLAMS. We are grateful for the excellent support provided by Theodore Bugtong, Jay Brown, George Postell, and many others at the NASA Wallops Flight Facility. We thank Fred Rose, John Murray, Louis Nguyen, and Dave Rutan who provided outstanding weather forecasts and Web support. The work of R. Kahn was carried out at the Jet Propulsion Laboratory, California Institute of Technology, under contract with the National Aeronautics and Space Administration. It is supported in part by the EOS-MISR instrument program, and by the NASA Earth Sciences Division Climate and Radiation Research and Analysis Program. MPL data provided by E. J. Welton and the NASA Micro-Pulse Lidar Network (MPLnet) are funded by the NASA Earth Observing System and the Radiation Sciences Program. AERONET data were provided by B. N. Holben and the NASA AERONET project. The participation of the University of Washington team and its Convair 580 aircraft was supported by grants from NASA and NSF.

REFERENCES

Bates, T. S., B. J. Huebert, J. L. Gras, F. B. Griffiths, and P. A. Durkee, 1998: International Global Atmospheric Chemistry (IGAC) project's first aerosol characterization experiment (ACE 1): Overview. *J. Geophys. Res.,* **103,** 16 297–16 318.

Bruegge, C. J., W. Abdou, D. J. Diner, B. J. Gaitley, M. Helmlinger, R. A. Kahn, and J. V. Martonchik, 2004: Validating the MISR radiometric scale for the ocean aerosol science communities. *Post-Launch Calibration of Satellite Sensors*, S. A. Morain and A. M. Budge, Eds., A. A. Balkoma, 103–115.

Castanho, A. D. A., J. V. Martins, P. V. Hobbs, P. Artaxo, L. Remer, and M. Yamasoe, 2005: Chemical characterization of aerosols on the East Coast of the United States using aircraft and ground-based stations during the CLAMS experiment. *J. Atmos. Sci.,* **62,** 934–946.

Charlock, T. P., F. G. Rose, D. Rutan, Z. Jin, D. Fillmore, and W. Collins, 2004: Global retrievals of the surface and atmosphere radiation budget and direct aerosol forcing. *Proc. 13th Conf. on Satellite Meteorology and Oceanography,* Norfolk, VA, Amer. Meteor. Soc., CD-ROM, P8.11.

Chowdhary, J., and Coauthors, 2005: Retrieval of aerosol scattering and absorption properties from photopolarimetric observations over the ocean during the CLAMS experiment. *J. Atmos. Sci.,* **62,** 1093–1117.

Collins, W. D., P. J. Rasch, B. E. Eaton, B. V. Khattatov, J. F. Lamarque, and C. S. Zender, 2001: Simulating aerosols using a chemical transport model with assimilation of satellite aerosol retrievals: Methodology for INDOEX. *J. Geophys. Res.,* **106,** 7313–7336.

Crowley, T. J., 2000: Causes of climate change over the past 1000 years. *Science,* **289,** 270–277.

Diner, D. J., and Coauthors, 1998a: Multiangle Imaging SpectroRadiometer (MISR)—Instrument description and experi-

ment overview. *IEEE Trans. Geosci. Remote Sens.,* **36,** 1072–1087.

——, and Coauthors, 1998b: The Airborne Multi-angle Imaging SpectroRadiometer (AirMISR): Instrument description and first results. *IEEE Trans. Geosci. Remote Sens.,* **36,** 1339–1349.

Dubovik, O., and M. D. King, 2000: A flexible inversion algorithm for retrieval of aerosol optical properties from sun and sky radiance measurements. *J. Geophys. Res.,* **105,** 20 673–20 696.

Gao, B. C., Y. J. Kaufman, D. Tanre, and R. R. Li, 2002: Distinguishing tropospheric aerosols from thin cirrus clouds for improved aerosol retrievals using the ratio of 1.38-μm and 1.24-μm channels. *Geophys. Res. Lett.,* **29,** 1890, doi:10.1029/2002GL015475.

Gatebe, C. K., M. D. King, A. I. Lyapustin, G. T. Arnold, and J. Redemann, 2005: Airborne spectral measurements of ocean directional reflectance. *J. Atmos. Sci.,* **62,** 1072–1092.

Holben, B. N., and Coauthors, 1998: AERONET—A federated instrument network and data archive for aerosol characterization. *Remote Sens. Environ.,* **66,** 1–16.

Houghton, J. T., Y. Ding, D. J. Griggs, M. Noguer, P. J. van der Linden, and D. Xiaosu, Eds., 2001: *Climate Change 2001: The Scientific Basis*. Cambridge University Press, 944 pp.

Huebert, B. J., T. Bates, P. B. Russell, G. Y. Shi, Y. J. Kim, K. Kawamura, G. Carmichael, and T. Nakajima, 2003: An overview of ACE-Asia: Strategies for quantifying the relationships between Asian aerosols and their climatic impacts. *J. Geophys. Res.,* **108,** 8633, doi:10.1029/2003JD003550.

Jin, Z., T. P. Charlock, and C. K. Rutledge, 2002: Analysis of broadband solar radiation and albedo over the ocean surface at COVE. *J. Atmos. Oceanic Technol.,* **19,** 1585–1601.

——, and Coauthors, 2005: Radiative transfer modeling for the CLAMS experiment. *J. Atmos. Sci.,* **62,** 1053–1071.

Kahn, R., P. Banerjee, D. McDonald, and D. J. Diner, 1998: Sensitivity of multiangle imaging to aerosol optical depth and to pure-particle size distribution and composition over ocean. *J. Geophys. Res.,* **103,** 32 195–32 213.

——, ——, and ——, 2001: Sensitivity of multiangle imaging to natural mixtures of aerosols over ocean. *J. Geophys. Res.,* **106,** 18 219–18 238.

——, and Coauthors, 2005: MISR calibration, and implications for low-light-level aerosol retrieval over dark water. *J. Atmos. Sci.,* **62,** 1032–1052.

Kaufman, Y. J., J. V. Martins, L. A. Remer, M. R. Schoeberl, and M. A. Yamasoe, 2002: Satellite retrieval of aerosol absorption over the oceans using sunglint. *Geophys. Res. Lett.,* **29,** 1928, doi:10.1029/2002GL015403.

Kindel, B. C., Z. Qu, and A. F. H. Goetz, 2001: Direct solar spectral irradiance and transmittance measurements from 350 to 2500 nm. *Appl. Opt.,* **40,** 3483–3494.

King, M. D., M. G. Strange, P. Leone, and L. R. Blain, 1986: Multiwavelength scanning radiometer from airborne measurements of scattered radiation within clouds. *J. Atmos. Oceanic Technol.,* **3,** 513–522.

——, Y. J. Kaufman, W. P. Menzel, and D. Tanre, 1992: Remote-sensing of cloud, aerosol, and water-vapor properties from the Moderate Resolution Imaging Spectrometer (MODIS). *IEEE Trans. Geosci. Remote Sens.,* **30,** 2–27.

——, and Coauthors, 1996: Airborne scanning spectrometer for remote sensing of cloud, aerosol, water vapor, and surface properties. *J. Atmos. Oceanic Technol.,* **13,** 777–794.

——, and ——, 2003: Cloud and aerosol properties, precipitable water, and profiles of temperature and water vapor from MODIS. *IEEE Trans. Geosci. Remote Sens.,* **41,** 442–458.

Levy, R. C., L. A. Remer, J. V. Martins, Y. J. Kaufman, A. Plana-Fattori, J. Redemann, P. B. Russell, and Wenny, B., 2005: Evaluation of the MODIS aerosol retrievals over ocean and land during CLAMS. *J. Atmos. Sci.,* **62,** 974–992.

Li, Z. Q., M. C. Cribb, and A. P. Trishchenko, 2002: Impact of surface inhomogeneity on solar radiative transfer under overcast conditions. *J. Geophys. Res.,* **107,** 4297, doi:10.1029/2001JD000976.

Loeb, N. G., N. Manalo-Smith, S. Kato, W. F. Miller, S. K. Gupta, P. Minnis, and B. A. Wielicki, 2003: Angular distribution models for top-of-atmosphere radiative flux estimation from the Clouds and the Earth's Radiant Energy System instrument on the Tropical Rainfall Measuring Mission satellite. Part I: Methodology. *J. Appl. Meteor.,* **42,** 240–265.

Magi, B., P. V. Hobbs, T. W. Kirchstetter, I. T. Novakov, D. A. Hegg, S. Gao, J. Redemann, and B. Schmid, 2005: Aerosol properties and chemical apportionment of aerosol optical depth at locations off the United States East Coast in July and August 2001. *J. Atmos. Sci.,* **62,** 919–933.

Mann, M. E., R. S. Bradley, and M. K. Hughes, 1999: Northern Hemisphere temperatures during the past millennium: Inferences, uncertainties, and limitations. *Geophys. Res. Lett.,* **26,** 759–762.

Martonchik, J. V., D. J. Diner, R. A. Kahn, T. P. Ackerman, M. E. Verstraete, B. Pinty, and H. R. Gordon, 1998: Techniques for the retrieval of aerosol properties over land and ocean using multiangle imaging. *IEEE Trans. Geosci. Remote Sens.,* **36,** 1212–1227.

——, ——, K. A. Crean, and M. A. Bull, 2002: Regional aerosol retrieval results from MISR. *IEEE Trans. Geosci. Remote Sens.,* **40,** 1520–1531.

Ohmura, A., and Coauthors, 1998: Baseline Surface Radiation Network (BSRN/WCRP): New precision radiometry for climate research. *Bull. Amer. Meteor. Soc.,* **79,** 2115–2136.

Raes, F., T. Bates, F. McGovern, and M. van Liedekerke, 2000: The 2nd Aerosol Characterization Experiment (ACE-2): General overview and main results. *Tellus,* **52B,** 111–125.

Redemann, J., and Coauthors, 2005: Suborbital measurements of spectral aerosol optical depth and its variability at subsatellite grid scales in support of CLAMS 2001. *J. Atmos. Sci.,* **62,** 993–1007.

Remer, L. A., and Coauthors, 2005: The MODIS aerosol algorithm, products, and validation. *J. Atmos. Sci.,* **62,** 947–973.

Russell, P. B., P. V. Hobbs, and L. L. Stowe, 1999: Aerosol properties and radiative effects in the United States East Coast haze plume: An overview of the Tropospheric Aerosol Radiative Forcing Observational Experiment (TARFOX). *J. Geophys. Res.,* **104,** 2213–2222.

Schmid, B., and Coauthors, 2003: Coordinated airborne, spaceborne, and ground-based measurements of massive thick aerosol layers during the dry season in southern Africa. *J. Geophys. Res.,* **108,** 8496, doi:10.1029/2002JD002297.

Smith, W. L., W. F. Feltz, R. O. Knuteson, H. E. Revercomb, H. B. Howell, and H. M. Woolf, 1999: The retrieval of planetary boundary layer structure using ground-based infrared spectral radiance measurements. *J. Atmos. Oceanic Technol.,* **16,** 323–333.

Smith, W. L., Sr., D. K. Zhou, A. M. Larar, S. A. Mango, H. B. Howell, R. O. Knuteson, H. E. Revercomb, and W. L. S. Smith Jr., 2005: The NPOESS Airborne Sounding Testbed Interferometer—Remotely sensed surface and atmospheric conditions during CLAMS. *J. Atmos. Sci.,* **62,** 1118–1134.

Su, W., T. P. Charlock, and C. K. Rutledge, 2002: Observations of reflectance distribution around sunglint from a coastal ocean platform. *Appl. Opt.,* **41,** 7369–7383.

Swap, R. J., and Coauthors, 2002: The Southern African Regional Science Initiative (SAFARI 2000): Overview of the dry season field campaign. *South Afr. J. Sci.,* **98,** 125–130.

Twomey, S., 1977: Influence of pollution on shortwave albedo of clouds. *J. Atmos. Sci.,* **34,** 1149–1152.

U.S. Bureau of the Census, cited 2004: International Data Base.

[Available online at http://www.census.gov/ipc/www/world.html.]

Welton, E. J., J. R. Campbell, J. D. Spinhirne, and V. S. Scott, 2001: Global monitoring of clouds and aerosols using a network of micropulse lidar systems. Vol. 4153, *Proc. Lidar Remote Sensing for Industry and Environmental Monitoring,* Sendai, Japan, SPIE, 151–158.

Wielicki, B. A., B. R. Barkstrom, E. F. Harrison, R. B. Lee, G. L. Smith, and J. E. Cooper, 1996: Clouds and the Earth's Radiant Energy System (CERES): An Earth Observing System experiment. *Bull. Amer. Meteor. Soc.,* **77,** 853–868.

——, and Coauthors, 2002: Evidence for large decadal variability in the tropical mean radiative energy budget. *Science,* **295,** 841–844.

Wolfe, D. E., and S. I. Gutman, 2000: Developing an operational, surface-based, GPS, water vapor observing system for NOAA: Network design and results. *J. Atmos. Oceanic Technol.,* **17,** 426–440.